The Mars Science Laboratory EDL Communications Brownout and Blackout at UHF

David D. Morabito,* Brian Schratz,† Kris Bruvold,† Peter Ilott,† Karl Edquist,‡ and Alicia Dwyer Cianciolo‡

ABSTRACT. — This article discusses the analysis of the UHF communications blackout (and brownout) experienced by the Mars Science Laboratory (MSL) during the period around peak heating of its entry, descent, and landing (EDL) phase into the Martian atmosphere on August 6, 2012. The UHF relay links from MSL to the Mars Reconnaissance Orbiter (MRO) and to the Mars Express (MEX) suffered a period of ~70 s of degradation, consisting of a combination of brownout (signal fades) and blackout (complete loss of signal) that coincided with the predicted period of signal degradation from preflight analyses. The observed signal fades and outages on both signal links spanned the interval from ~30 s to ~95 s after entry at the atmospheric interface. This article discusses both predictions and measurements of signal degradation that occurred during the peak heating phase of the MSL EDL.

I. Introduction

A spacecraft will become enveloped by ionized particles due to dissociation and subsequent ionization of atmospheric gases as they are heated during entry into a planetary atmosphere at hypersonic velocities. When the electron number density, traversing the signal path between transmitting probe and receiving asset, becomes sufficiently high, radio communications can become disrupted. This degradation takes the form of either fades (brownout) or total loss (blackout) as signal energy is reflected or absorbed by the intervening charged particles [1].

Earlier work involving an analysis of entry vehicles into the Martian atmosphere included a postflight study of the 30-s signal outage suffered by the Mars Pathfinder spacecraft in 1997 at X-band on a direct-to-Earth (DTE) link, attributed mostly to charged particles [2]. Other previous work included predictions of no blackout during atmospheric entry of the Mars Exploration Rovers in 2004 at X-band [2] and predictions and postflight analysis of signal degradation for Phoenix Mars Lander during atmospheric entry in 2008 at UHF [1]. Mars Pathfinder had the highest entry velocity among the Mars entry probes (7.5 km/s), resulting

* Communications Architectures and Research Section.
† Flight Communications Section.
‡ NASA Langley Research Center, Hampton, Virginia.

The research described in this publication was carried out by the Jet Propulsion Laboratory, California Institute of Technology, under a contract with the National Aeronautics and Space Administration.

in the 30-s blackout at X-band. The two Mars Exploration Rovers entered the Martian atmosphere at much lower entry velocities of ~5.5 km/s, in which no degradation was observed at X-band, as was predicted [2].

The Phoenix Mars Lander was launched on August 4, 2007, and landed in the north polar region of Mars on May 25, 2008. A sophisticated strategy was employed for the critical entry, descent, and landing (EDL) phase of the mission [3,4]. During entry, the UHF carrier emitted by Phoenix was received and recorded by three orbiting relay spacecraft and then transmitted to NASA's Deep Space Network (DSN) tracking stations via the DTE telemetry link. The received signal data from each link were analyzed in time and frequency. In addition, the Phoenix UHF carrier was received on a DTE link to the National Radio Astronomy Observatory (NRAO) 100-m-diameter antenna in Green Bank, West Virginia [1].

Previous studies suggested that there was a greater potential for a communications blackout during peak heating at the UHF frequency (~401 MHz) used for orbiting Mars relay links [1,2]. Preflight work on the Phoenix EDL entry at Mars to characterize any communication degradation at its UHF link frequency was performed and documented in internal reports cited in [1]. Prior to EDL, the preflight predictions suggested a 1 ± 1 min outage period centered about peak heating. The outage period was thus predicted to range from no outage (0 s) to a maximum of 2 min, assuming conservative bounds of uncertainties believed to be the case during early preflight analysis. These bounds were based on most-favorable and worst-case assumptions of the Phoenix entry parameters, as there was no specific orbiter relay link trajectory information available at the time. Several trajectories with atmospheric entry velocities of up to 5.8 km/s were considered. Aerothermodynamic analyses programs such as NASA Langley's LAURA (Langley Aerothermodynamic Upwind Relaxation Algorithm) program [5] were used to estimate the electron number density profile about the vehicle for different entry scenarios.

Phoenix entered the Martian atmosphere on May 25, 2008, and did not suffer a signal outage (blackout) to any of the three orbiter relay links during the period around peak heating. The preliminary electron number density profile estimates about the vehicle used for the worst-case predictions were based on a higher entry velocity (5.8 km/s) than was actually flown (5.6 km/s). However, during postflight analysis, a close inspection of the received signal data revealed significant fades (brownout) that coincided with high levels of electrons that enveloped the spacecraft during the period about peak heating, as predicted by aerothermodynamic entry analysis. By comparing the maximum electron number density that the signal path crosses in a LAURA-output contour plot against the critical electron number density for the link frequency, one can infer whether there is a potential for degradation or blackout. The postflight analysis for Mars Pathfinder and predictions for the Mars Exploration Rovers [2] assumed an "on–off switch" (no attenuation versus total signal outage). For Phoenix, the electron number density profile along the signal path marginally exceeded the threshold electron number density for degradation at UHF that was not so high that it did not cause blackout. Thus, given that the electron number density profiles were marginally above the threshold and all three orbiter relay links had significant signal-to-noise ratio (SNR), the signal fades were easily measurable and allowed comparison with predicted fades based on LAURA electron number density profiles [1].

The work on predicting signal degradation for Mars Science Laboratory (MSL) atmospheric entry began ~2004 and involved the analysis of two different trajectories at 6.3 km/s and 5.7 km/s at the atmospheric entry interface [6]. The conclusion of an initial study was that one would expect a degradation of up to 100 s at UHF (401 MHz) frequencies and no degradation at the X-band (8.4 GHz) DTE link [6]. The MSL EDL communications analysis was revisited in 2010 and 2012 using an entry trajectory with a 5.9 km/s entry velocity. The conclusion, as documented in internal JPL reports, suggested that any UHF degradation would last up to a maximum of 70 s and be as short as 0 s, and that there would be no degradation on the X-band DTE link.

In this article, we will analyze the entry trajectory that was flown for the MSL EDL (Section II), examine preflight signal degradation predictions for MSL EDL (Section III), examine received signal-level data during the predicted signal degradation period and compare any signal outages or fades with the predicted degradation periods (Section IV), and compare trends of the predicted signal degradation signature with the measured signal degradation signature (Section V). Finally, we offer some concluding remarks (Section VI).

II. Trajectory Analysis

Several years prior to the MSL EDL, a set of prospective entry trajectories for different candidate landing sites was considered [7] with entry velocities ranging from the most stressful (6.26 km/s) to less stressful (5.7 km/s) [6]. The "final" planned MSL entry trajectory had an entry velocity of ~5.9 km/s.

Figure 1 displays atmospheric relative velocity and neutral atmospheric density profiles for Phoenix and MSL for the time span from atmospheric entry at 0 s to 160 s past entry. The point of atmospheric entry boundary for Mars is defined as a planet-centered spherical shell with a radius of 3522.2 km from the center of the planet (~128 km altitude for Phoenix and ~124 km for MSL). The vertical dashed purple lines at 60 s and 110 s denote the extent of the period of observed Phoenix UHF signal degradation on all three orbiting relay links during EDL on May 25, 2008 [1]. The observed MSL UHF degradation window started earlier than that of Phoenix and spanned from ~30 s to ~95 s past entry (depicted by dashed dark blue vertical lines). Since received signal degradation due to charged particles depends on the combination of atmospheric relative velocity and atmospheric density, one can see upon examination of Figure 1 that the start of each degradation period occurred at similar velocities and similar densities for both spacecraft. However, although the end of the degradation periods was marked by very different velocities (Phoenix was faster) and very different densities (MSL's was denser), it is the combination that is important in the generation of free electrons. The actual outage period for each entry scenario is hence mostly dependent on the combination of relative velocity and atmospheric density, which thus determines the number of free electrons generated along the signal path.

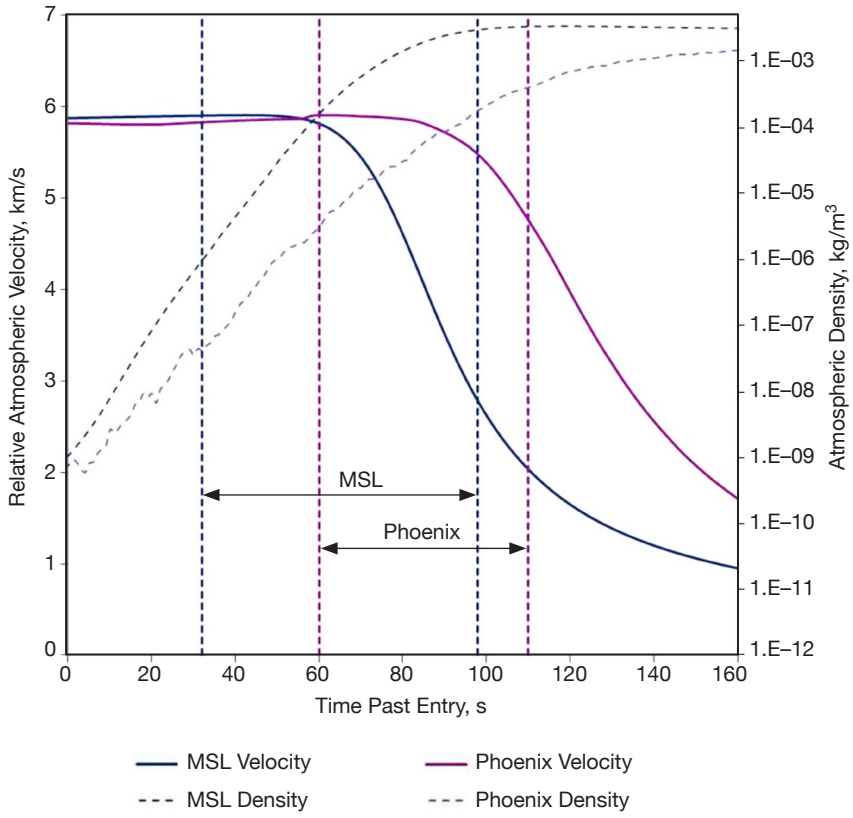

Figure 1. Phoenix and MSL Mars entry relative velocity (linear) and neutral atmospheric density (log) profiles relative to time past atmospheric entry. The observed UHF signal degradation periods for Phoenix and MSL during their respective periods around peak heating are annotated on the plot.

If we shift the Phoenix time tags such that the start of the two outages occurs at the same time on the x-axis, we obtain the plot shown in Figure 2. The combination of the entry velocity and atmospheric density pairs at the start of the degradation periods will produce similar electron number densities for both Phoenix and MSL using parametric models [2]. In addition, the Phoenix relative velocity and atmospheric density pair at the end of its degradation period will produce a similar electron number density using the MSL relative velocity and atmospheric density at the end of the MSL degradation period per the parametric models. The entry profiles were used in the generation of the preflight predictions of degradation using both parametric models and aerothermodynamic tools such as Horton and LAURA [1]. In actuality, the degree of actual degradation will also depend on the direction of the relay asset relative to the vehicle, and the placement of the antenna on the vehicle (Section V).

The MSL Mars relative velocity is based on a navigation filter reconstruction[1,2] that utilized inertial measurement unit (IMU) data to obtain a postflight estimate of the entry trajec-

[1] J. L. Davis, "MSL Reconstructed POST2 Variable Descriptions and Assumptions," Interoffice Memorandum IOM-D205-JLD-2012-004 (internal document), NASA Langley Research Center, Hampton, Virginia, November 15, 2012.

[2] A. Chen, A. Dwyer Cianciolo, A. Vasavada, C. Karlgaard, J. Barnes, B. Cantor, D. Kass, S. Rafkin, and D. Tyler, "Reconstruction of Atmospheric Properties from the Mars Science Laboratory Entry, Descent, and Landing," *AIAA Journal of Spacecraft and Rockets*, 2014 (in press).

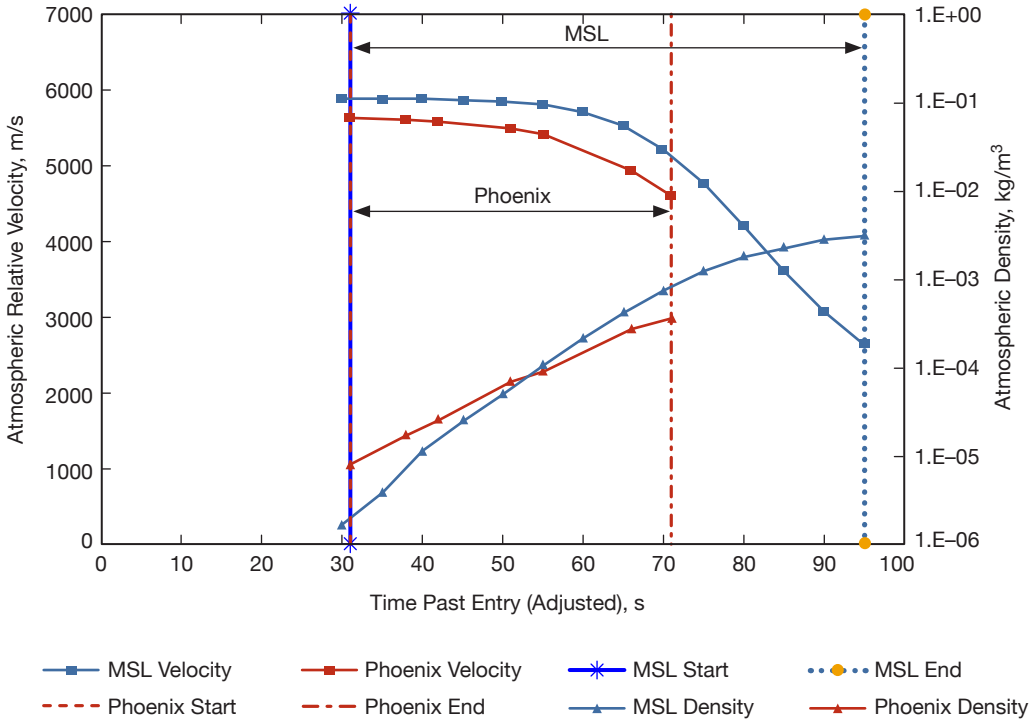

Figure 2. Mars entry relative velocity (linear) and neutral atmospheric density (log) profiles relative to "adjusted" time past atmospheric entry (Phoenix time scale shifted so that both degradation periods start at same time). Also shown are the observed "approximate" UHF signal degradation periods for Phoenix and MSL.

tory (position and velocity). Neutral atmosphere density is based on the reconstructed atmosphere profile that includes data from the Mars Reconnaissance Orbiter's (MRO's) Mars Climate Sounder (MCS), the Mars Entry Atmosphere Data System (MEADS) portion of MSL's Mars EDL Instrument (MEDLI) suite and postflight mesoscale models.[3] The relative velocity and neutral atmospheric density at selected time stamps during entry are used as inputs in aerothermodynamic tools to generate electron number densities used in postflight analysis of observed signal degradation. No effort was put forth to reconstruct winds in this model as they were not expected to significantly affect the velocities, which in turn affect the estimation of charged particle density.

III. Preflight Signal Degradation Predictions

Figure 3 displays predicted preflight electron number densities from LAURA (colored points) as a function of time past entry interface based on the MSL entry trajectory designated as 09-TPS-02, as well as parametric curves based on the trajectory. Preflight spot checks (black points) that were estimated in 2012 using an updated similar trajectory were found to be reasonably consistent with the parametric models described in [2]. The preflight atmosphere model[4] did not yet include the refinements used in the reconstructed trajectory for

[3] Ibid.

[4] Ibid.

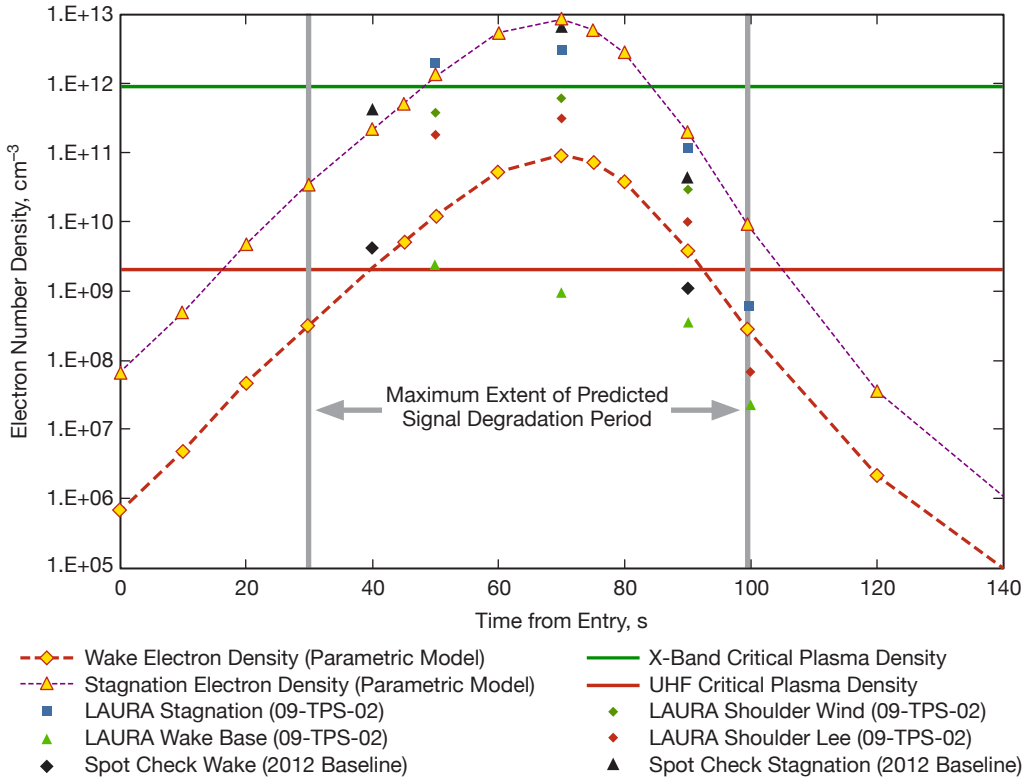

Figure 3. Predicted electron number density as a function of time past entry for MSL entry trajectories in different directions from the vehicle. The likely worst-case degradation period for UHF spanned from about 30 s to 100 s, based on conservative extrapolation of shoulder electron number density signatures for likely cone angles.

the post-EDL analysis. The final reconstructed trajectory used in the Section V analysis included significant changes in atmospheric relative velocity and neutral atmospheric density for altitudes below 50 km. The peak heating rate occurring between 65 s and 80 s past entry corresponds to the period of highest predicted peak electron number density, as seen in the peak of the parametric curves shown in Figure 3.

From the Phoenix EDL analysis where the relay assets were located at cone angles near 90 deg, we expected that the electron number densities were overestimated during much of the degradation period [1]. Based on this assumption, the likely worst-case MSL degradation period at UHF for ~90 deg cone angles spanned from 30 s to 100 s past entry, using a conservative extrapolation of electron number densities in the shoulder direction (90 deg wind-side and lee-side). The wind-side and lee-side shoulder estimates were thus extrapolated down to the UHF threshold (thick red horizontal line) using the two parametric model curves as a guide. We thus expected a worst-case degradation period of ~70 s at UHF for cone angles ~90 deg to any relay assets, as documented in internal JPL reports.

For the case of relay assets that lie in the direction behind the vehicle, we examined the wake direction estimates. Given the LAURA base estimates shown in Figure 3, we see only one point that lies on the UHF threshold curve and all others points lie below it. Hence, for

the best case at UHF we would had expected no degradation (0 s degradation period) for any relay asset lying in that direction. It is cautioned that the wake region parametric model that lies above these estimates is fairly conservative and served as a worst-case estimate.

All LAURA shoulder and base estimates lie below the X-band threshold for signal degradation (thick green line). We therefore did not expect charged-particle degradation to any MSL X-band DTE signal links.

IV. Measured Signal Degradation and Comparison with Preflight Predictions

During EDL, MSL transmitted signal energy to three relay Mars orbiting spacecraft at UHF and to ground stations via a DTE link at X-band. During the period around peak heating, the receivers on board the MRO and Mars Express (MEX) orbiters achieved lock and signal visibility at UHF and hence the received signal was recorded on board the spacecraft. The Mars Odyssey spacecraft did not have telemetry lock until after the period of charged-particle degradation and hence the MSL-to-Odyssey link will not be further discussed. The MSL DTE link did not suffer any degradation at X-band as was predicted for the period around peak heating, as the higher frequency is less susceptible to the effects of charged particles [8,9].

The UHF signal emitted by MSL was received by MRO's Electra radio. The in-phase and quadrature components of the signal were recorded on board MRO in open-loop fashion. These signal data were relayed to a NASA DSN antenna on Earth over MRO's DTE X-band telemetry link. The spectra extracted from the open-loop data as a function of time were examined and processed at different bandwidths to extract carrier-to-noise ratio (CNR) and frequency estimates. Figure 4 displays the received CNR based on processing of the recorded signal data using a bandwidth of ±30 Hz covering the full period around EDL. During time instances occurring at or near certain events, all of the signal energy went into the carrier and is visible in Figure 4 as 5 db to 6 dB "spikes." Such events include bank reversal maneuver events and parachute deployment. Events such as the plasma degradation period and parachute deployment are annotated on Figure 4. The carrier-only pulses were correlated with the timing of known events and allowed us to translate the recorded time tags to those of other time frames, in particular, time relative to the entry at the atmospheric interface. Therefore, t = 0 s on the horizontal axis in Figure 4 is defined when MSL was 3522.2 km from the center of Mars.

Figure 5 displays the MSL-to-MRO received signal levels for the ±30 Hz bandwidth spectral processing from Figure 4 about the period immediately surrounding the plasma degradation from 0 s to 140 s past entry (light brown). Also shown in Figure 5 is the MSL-to-MRO received signal-level (CNR) signature based on processing about a ±100-Hz bandwidth (blue).

In addition, the signal-level data from MSL to MEX are also shown in Figure 5 (dark red squares). The received UHF signal from MSL was recorded on board MEX during EDL using 1-bit analog-to-digital (A/D) sampling (real component only) in a form known as "canister" data. The data were relayed to Earth stations via the X-band telemetry link on board MEX.

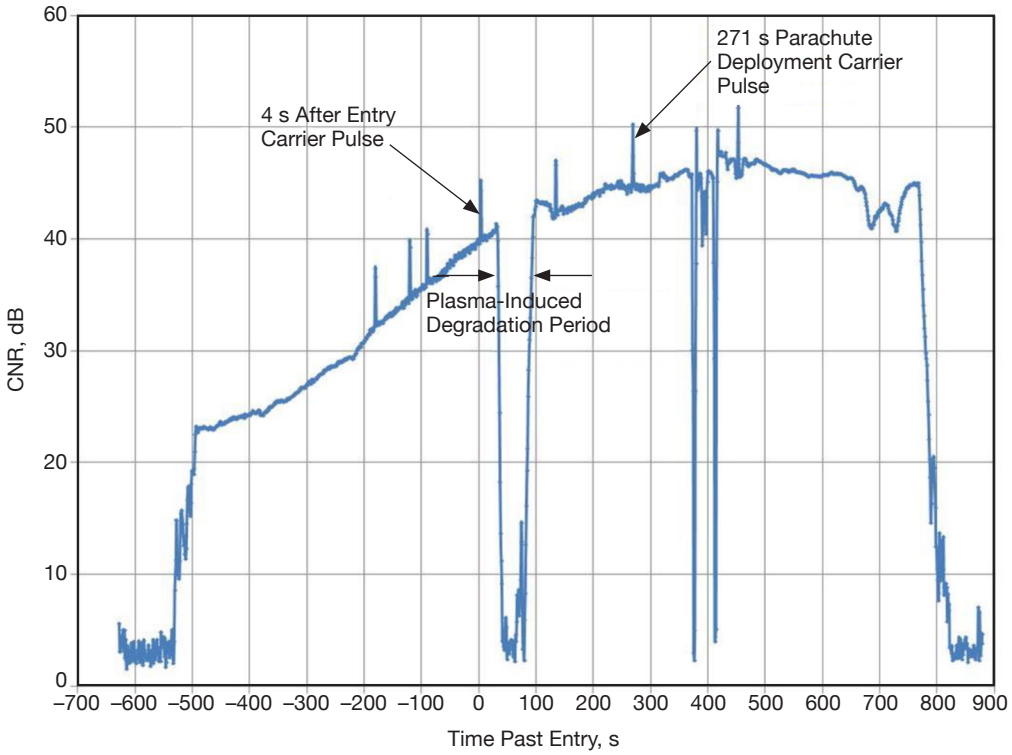

Figure 4. MRO received signal CNR ratio from MSL as measured from spectral processing of open-loop data using a ±30-Hz bandwidth. The plasma degradation period is shown on this plot occurring between ~30 s to ~100 s past entry. Also shown are carrier-only pulses that denote various events during EDL, such as parachute deployment at ~271 s past entry.

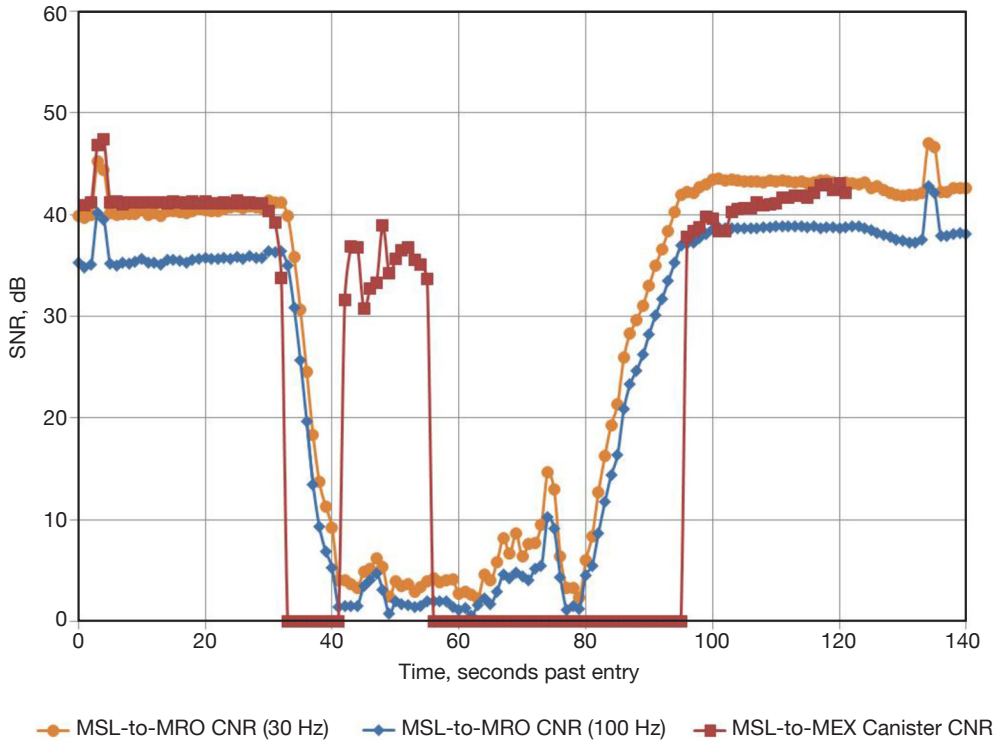

Figure 5. Received carrier SNR extracted from processing of the MSL-to-MRO and MSL-to-MEX signal link data for the period around plasma degradation.

These data were processed to produce a spectral representation of the received signal at a 42.096 kHz sampling rate. The carrier strength was then examined at selected time instances during EDL.

Figure 6 displays both the preflight electron number density estimates taken from Figure 3 (top) and the postflight measurements of signal CNR for both MSL–MRO and MSL–MEX links taken from Figure 5 (bottom). The predicted degradation period from the preflight analysis of Figure 3 in the form of solid vertical lines (top of Figure 6) were extended down into the postflight plot of received signal levels (bottom of Figure 6). The carrier-only spikes at 4 s and 136 s past entry in Figure 6 were used to align the time tags of the recorded signal-level data to the proper time reference relative to atmospheric entry that were also used in the electron number density plot. The predicted 70-s outage period extracted from the electron number density profiles (top of Figure 6) extending from 30 s to 100 s past entry aligns very well with the degradation period of the relay orbiter received signal levels (bottom of Figure 6). For the MSL-to-MRO signal link, this degradation period consists of a brownout period of decreasing CNR between roughly 30 s to 40 s, a "blackout" period between 40 s and 80 s where the CNR drops below 10 dB (except for a brief period at about 75 s where it lies just above 10 dB), and a brownout period of increasing CNR from ~82 s to ~100 s, where the signal level increases back to its undisturbed levels around 42 dB (for the ±30-Hz bandwidth case). The MSL–MEX signal-level estimates from the canister data show an abrupt signal drop near 30 s and an abrupt signal increase just before 100 s past entry, lining up well with the predicted degradation period except for a short period from ~40 s to ~55 s, where significant but still degraded signal energy was received. The line width of the carrier (from spectral processing) recovered between ~40 s to 55 s past entry was found to be broadened, consistent with the signal transiting blobs of plasma.

V. Reconstructed Trend Analysis

The LAURA Computational Fluid Dynamics (CFD) post-EDL analysis was performed to provide electron number density profiles about the MSL vehicle along predefined directions and later along actual signal path directions making use of clock and cone angles. The results from one analysis were used to compare the electron number density signatures for shoulder or wake directions against any observed signal degradation signatures during EDL. In addition, electron number density signatures were also generated along the signal line of sight to allow prediction of signal fades. These signal fades can then be compared against fades seen in the received signal SNR or CNR during the period around peak heating.

The LAURA software (Version: 050906 using OML-13F geometry) was run for chemical nonequilibrium and thermal nonequilibrium (two-temperature) conditions [5]. The Park-94 reaction rates [10] were used for 20 species (including free electrons) that resulted from an atmosphere with a free stream composition of 97 percent CO_2 and 3 percent N_2 by mass. Argon was neglected as it does not appreciably contribute to free electrons. An initial set of CFD solutions was generated at time instances of t = 35, 40, 45, 50, 55, 60, 65, 70, 75, 80, and 85 s after entry. These solutions provided insight on the magnitudes of the electron number density profile about the vehicle in specific directions. Figure 7 displays the LAURA

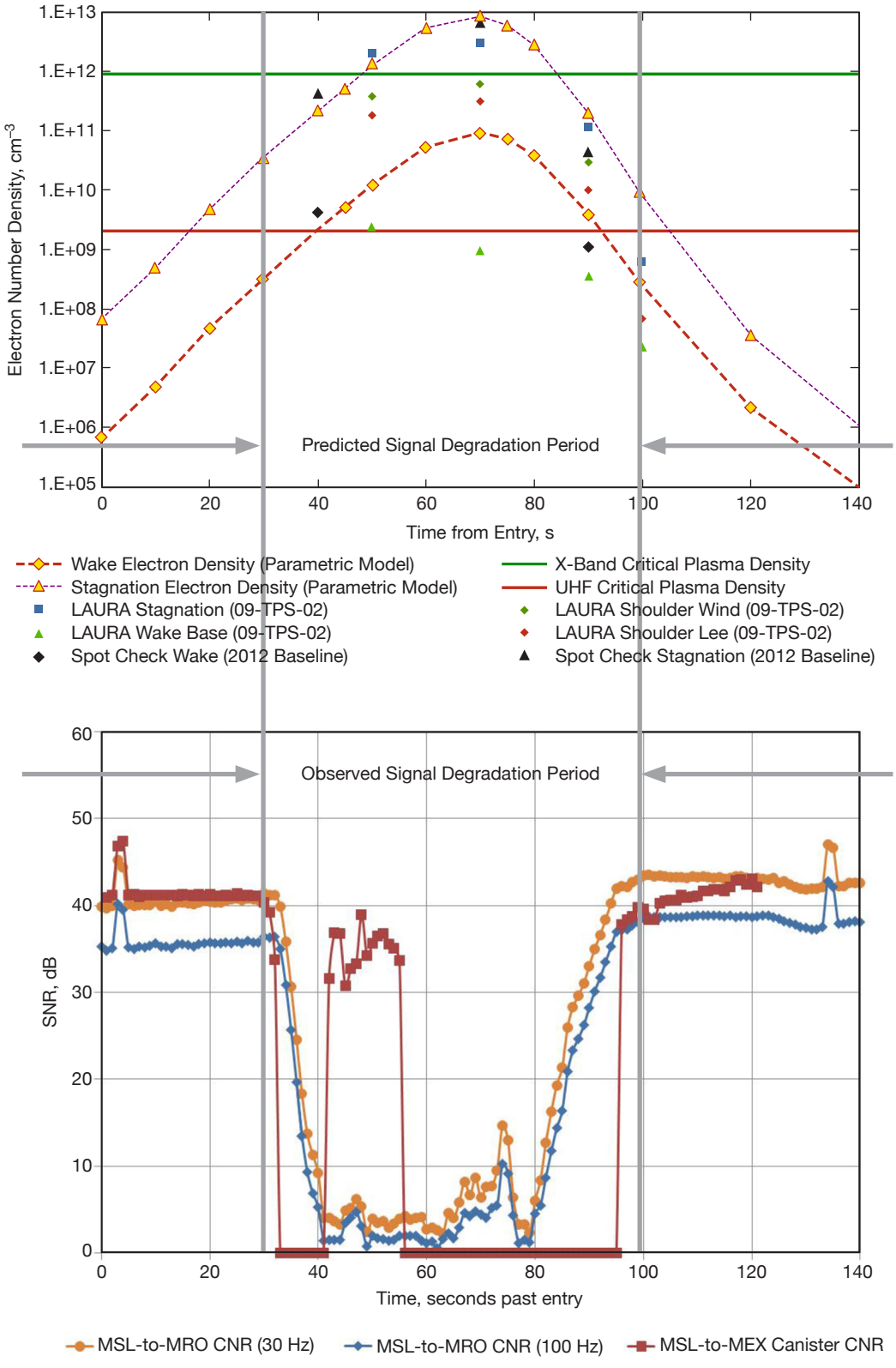

Figure 6. Preflight electron number density estimates (top) and the postflight measured signal-level data for both MSL–MRO and MSL–MEX links (bottom). The predicted preflight degradation period from ~30 s to ~100 s designated in the form of solid vertical lines on the electron density profile (top) were extended down into the postflight plot of received signal level (bottom).

electron number density profiles at these selected time tags for four different directions about the vehicle; nose (top left), windward direction (top right), leeward shoulder (bottom left), and wake direction (bottom right). The arrows on the vehicle diagram insets indicate the direction and location on the vehicle from which the profiles apply. For reference, the critical electron number density for signal degradation at the 401 MHz UHF frequency is 2×10^9 cm^{-3}. This threshold is exceeded for all cases except the wake direction case. The LAURA profiles in Figure 7 are reasonably consistent with the preflight results shown earlier in Figures 3 and 6 (top). The actual cone angles for the MSL-to-MRO signal link (see solid blue curve in Figure 8) lie near those of the windward and leeward shoulder directions, except they originate on the center ring of the transmitting parachute UHF (PUHF) antenna (see pink arrow in Figure 9). The cone angles for the MSL-to-MEX signal link lay predominately in the wake direction during the period around peak heating (see dashed blue curve in Figure 8).

In order to achieve a more accurate read on the expected signal degradation, electron number density profiles along the clock and cone angles about the vehicle in the directions to MRO and MEX were generated. The clock and cone angle signatures as a function of time for both signal links are shown in Figure 8. The LAURA program was run to extract the electron number density profiles along these signal links from the center ring of the transmitting PUHF antenna located on the backshell of the vehicle (see Figure 9 for the example of the MSL-to-MRO link at 35 s past entry). Estimates of signal attenuation were then extracted from the electron number density profiles using the approach documented in [1].

A. MSL-to-MRO Signal Link Analysis

Figure 10 displays two different views of the color-coded electron number density in the "extract plane" in which the MSL-to-MRO signal line of sight falls in a particular direction. Figure 10 (right) shows the extraction plane containing the direction of the signal path (denoted by the pink arrow) along with an illustration on how its clock angle is measured in the X–Y plane (counterclockwise about the Z-axis). Figure 9 shows a view of the cone angle definition, as previously discussed.

Figure 11 shows the electron number density profiles along the designated signal line of sight to MRO at the selected time tags from 35 s to 85 s. Notice that for almost all cases, the electron number density exceeds the UHF threshold (2×10^9 cm^{-3}), which implies signal degradation at these times. An additional solution was later performed for 30 s past entry.

LAURA electron number density solutions along the signal line of sight were performed every 5 s from 30 s to 85 s past entry, where the peak of each profile is shown in the light blue curve in Figure 12. LAURA solutions below 30 s were not feasible since the atmosphere is too rarified at the very high altitudes. Thus, we were unable to obtain reliable solutions at 20 s and 25 s past entry. However, one can visually extrapolate the green or light blue curves in Figure 12 to the left and infer that they would cross the threshold electron number density around these times and where no degradation is observed in the received MSL–MRO signal CNR data.

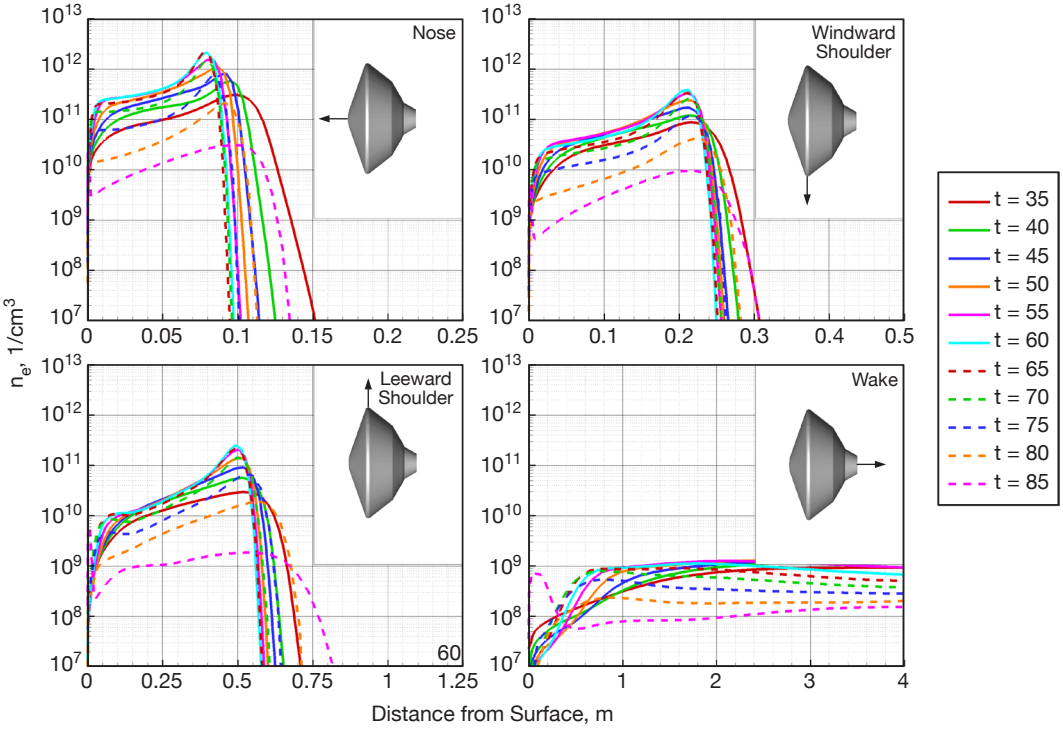

Figure 7. LAURA electron number density profiles at selected time tags from different directions about the vehicle: nose (top left), windward shoulder (top right), leeward shoulder (bottom left), and wake (bottom right).

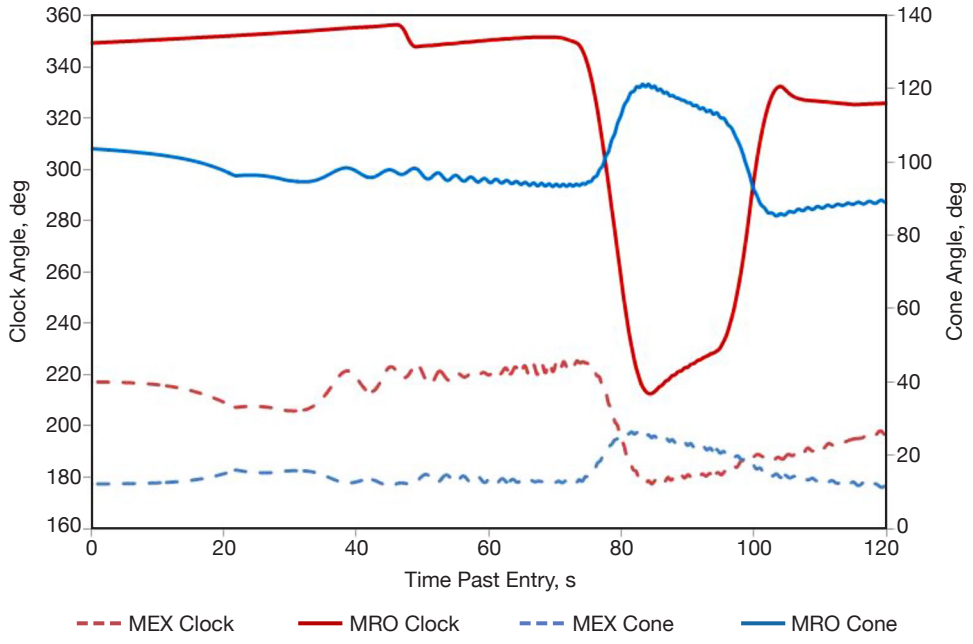

Figure 8. Clock (red) and cone (blue) angles about the MSL vehicle to direction of MRO (solid) and MEX (dashed).

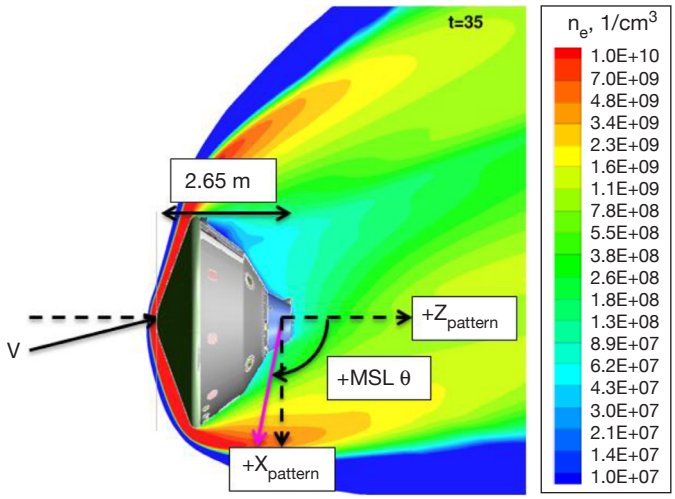

Figure 9. MSL vehicle embedded in color-coded electron number density plane with center ring of PUHF antenna serving as origin of signal link at 35 s past entry. The pink arrow extending outward from the center ring of the PUHF antenna denotes the direction to MRO. The cone angle θ is defined as the angular extent from the Z-axis to the direction of the relay link in the X–Z plane.

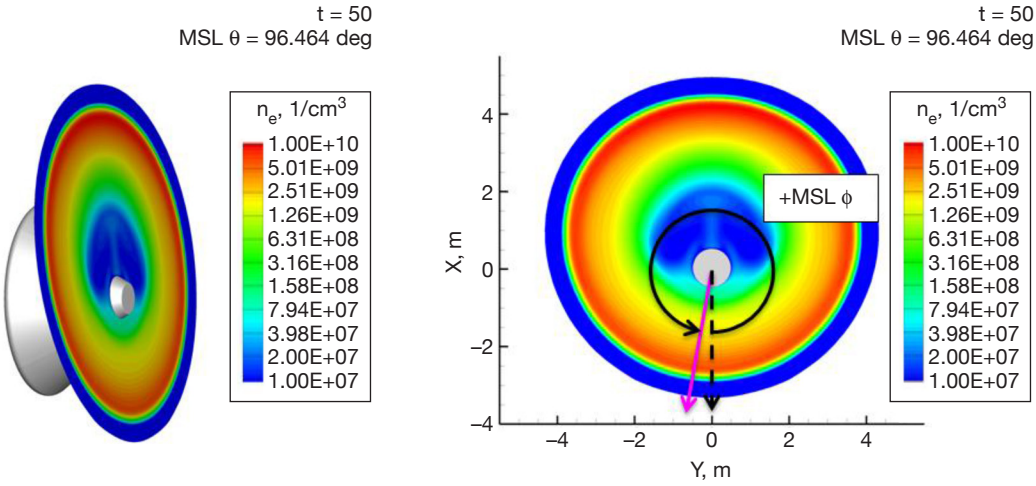

Figure 10. Extract plane (centered at ZLAURA = –2.65 m) defined by the angle "MSL θ" (left) at 50 s past entry. Extract line (pink arrow) for electron number density profile along signal line of sight in the LAURA X–Y plane defined by angle "MSL ϕ" as seen from vehicle rear (right). This clock angle is defined as a rotation in the X–Y plane about the vehicle Z-axis, counterclockwise as seen from the rear of the vehicle.

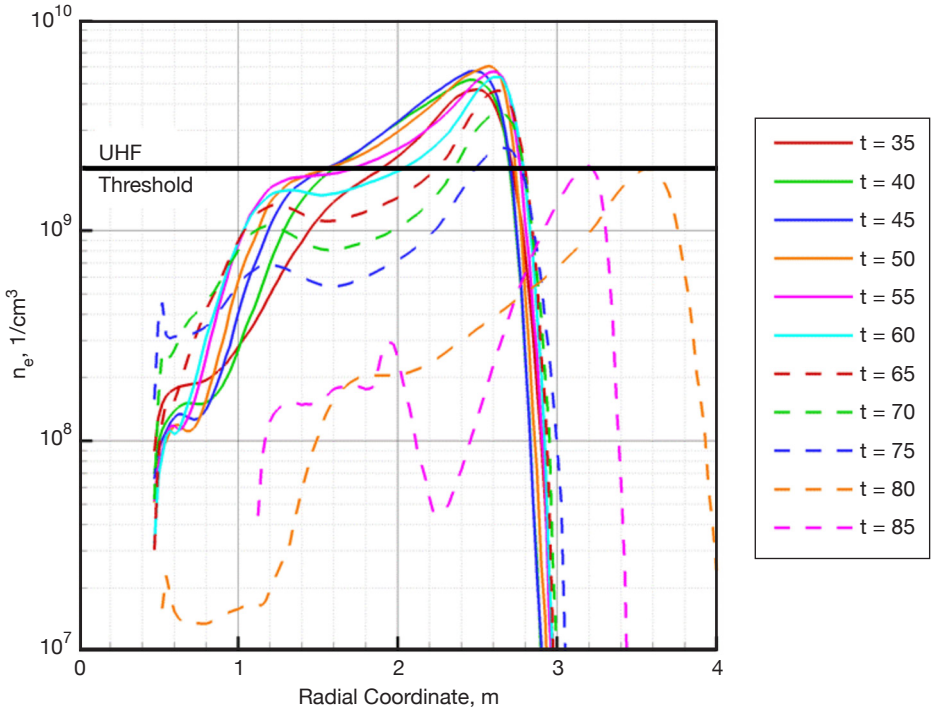

Figure 11. Electron number density profiles along the MSL-to-MRO signal link at each time instance. The radial coordinate origin is at XLAURA = YLAURA = 0. The maximum electron number density of 6.0×10^9 cm^{-3} occurs at t = 50 s.

Figure 12 is an expanded view of the received MSL-to-MRO CNR profile (brown) of Figure 6 (bottom) about the period around peak heating covering 0 s to 120 s past entry. Also shown are the signatures of the peak electron number density versus time for various directions discussed earlier, as well as the added curve of the peak electron number density along the cone angle line of sight. The profiles for the nose (blue diamonds), windward (red squares), leeward (light green triangles), and line of sight from PUHF (light blue) lie above the critical UHF electron number density (horizontal black line), and the wake region density (purple) lies below the UHF electron number density threshold required for signal degradation.

The red diamonds in Figure 12 denote the estimated CNR signal strength based on converting the electron number density profiles from LAURA at the selected time instances to attenuation using formulation provided by [1] (with γ set to unity in Equation 1 in [1]), and then translating the signal fades to predicted CNR by setting the 0 dB fade levels to match the measured signal CNR outside of the degradation period. This included adding a 41 dB background signal level to the fade values along with corrections for range distance changes and PUHF gain changes at each time tag estimate of the predicted signal level. The corrections to gain as a function of clock and cone angle were obtained from provided PUHF profiles[5] also published in [11] (see Figure 13). The three largest contributions of errors for predicted signal level (red diamonds) are uncertainty in LAURA electron number density (up to one magnitude depending on atmospheric realm), trajectory error, and uncertainty in PUHF antenna pattern used in the gain corrections (as the antenna pattern was not characterized in flight).

[5] P. Brown, personal communication, Jet Propulsion Laboratory, Pasadena, California, August 2013.

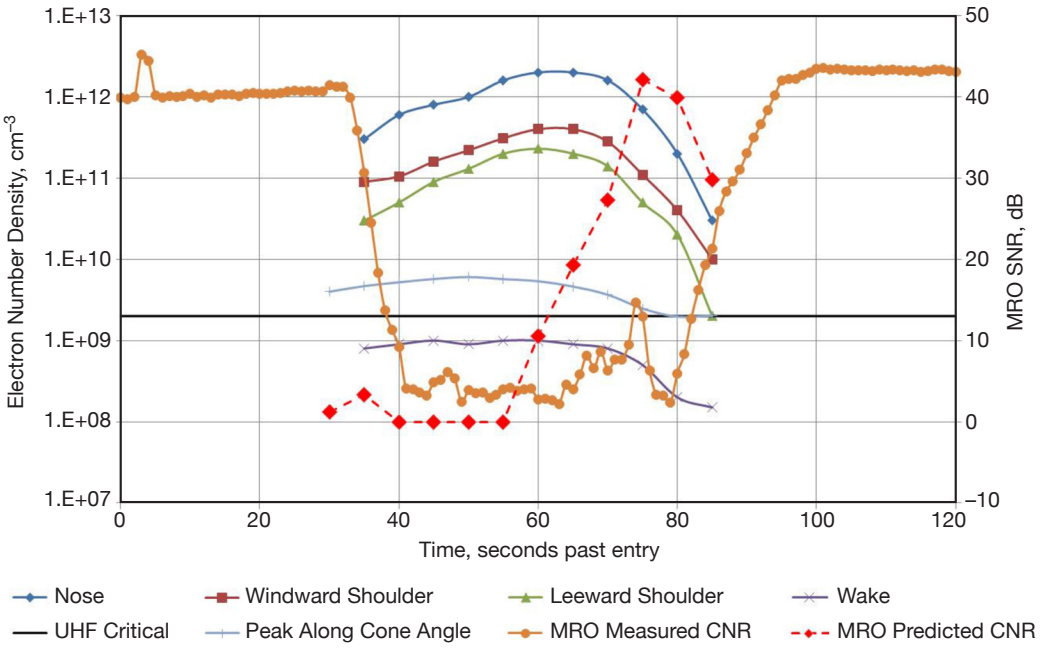

Figure 12. Received MSL-to-MRO CNR profile at ±30 Hz (brown) from Figure 6 (bottom) about the period around peak heating covering 0 s to 120 s past entry. Also shown are the peak electron number density signatures, including the peak along the line of sight (light blue curve) from the Langley LAURA analysis, and the predicted signal levels (red diamonds) discussed in the text.

The peak of the electron number density curve along the signal link (light blue curve in Figure 12) is shown to lie below the nose and shoulder curves and above the wake region curve, roughly aligning with the signal degradation period within the uncertainty of the LAURA electron number density estimates. Note that in Figure 12, during much of the signal degradation period, the peak electron number density along the signal path (light blue curve) lies above the threshold electron number density for UHF (2×10^9 cm^{-3}). Whenever the electron number density lies above the threshold, there is a possibility of significant signal degradation (either brownout or blackout), whereas when it falls below the threshold there will be no signal degradation. There is reasonable alignment of the predicted CNR extracted from the LAURA electron number density profiles and the measured CNR. We believe that during the first few seconds below 35 s, LAURA may be overestimating electron density [1] and becoming less overestimated (or underestimated) by the end of the degradation period (from ~70 s to ~85 s).

There are periods of both brownout and blackout in the measured CNRs between MSL and MRO during EDL in Figure 12. From 30 s to, roughly, 40 s after entry, the CNR is clearly detectable but decreasing (brownout), whereas between 40 s to roughly 80 s, the CNR lies mostly below 10 dB (sometimes peaking above 10 dB), denoting blackout. Between 80 s to roughly 100 s past entry, the CNR is increasing and detectable, denoting a period of brownout before the signal level returns to its nominal value free of charged-particle effects. The estimated signal levels (red diamonds) at 40 s, 45 s, 50 s, and 55 s have fade values that extend beyond or lie close to the noise floor consistent with the observed signal strengths

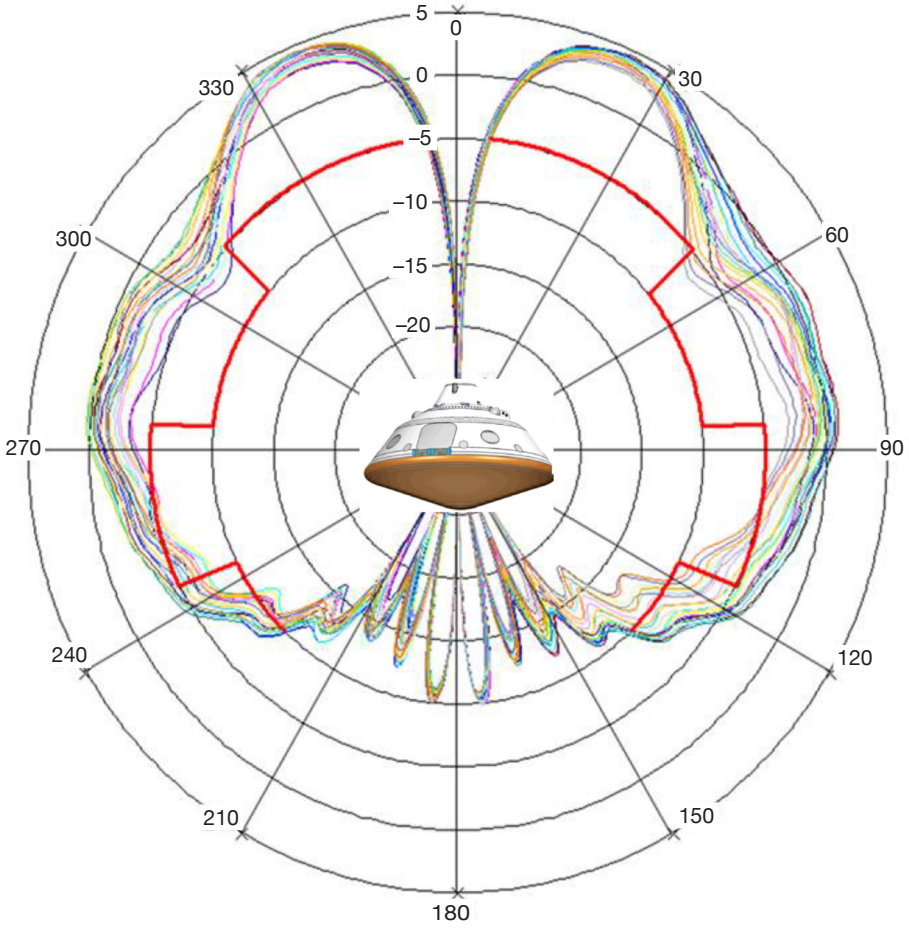

Figure 13. PUHF gain pattern in dB about vehicle as a function of cone angle, where each curve designates a different clock angle (from [11]).

for MSL–MRO, indicating blackout conditions. However, the predicted signal-level values from 65 s to 85 s rise well above the detectable CNR threshold, suggesting that the LAURA electron number density profiles are underestimated. The feature between 65 s and 85 s almost appears to be an amplified version that mimics the small CNR feature in the measured data that just peaks above 10 dB near 75 s.

The predicted signal levels at 30 s and 35 s in Figure 12 suggest blackout, whereas the actual signal-level profile shows a decreasing trend with sufficient SNR (brownout), suggesting that the electron number density estimates from LAURA are overestimated. Given that this regime is characterized with rarified atmospheric conditions, it is suggestive of high uncertainties in the LAURA model in this regime and perhaps also due to some degree of trajectory error, opposite that of the underestimation of electrons inferred from the higher value of the trend between 65 s and 85 s. This is supported in Figure 14, where the predicted signal levels (red diamonds) were made to agree with the observed signal-level data by appropriate setting of the adjustment factors (γ in Equation 1 in [1]) shown in Figure 15. The adjustment factors are less than unity at 30 s, 35 s, and 40 s, set to unity at 45 s to 55 s, and are higher than unity at time instances at and above 60 s. Thus, there is a generally increas-

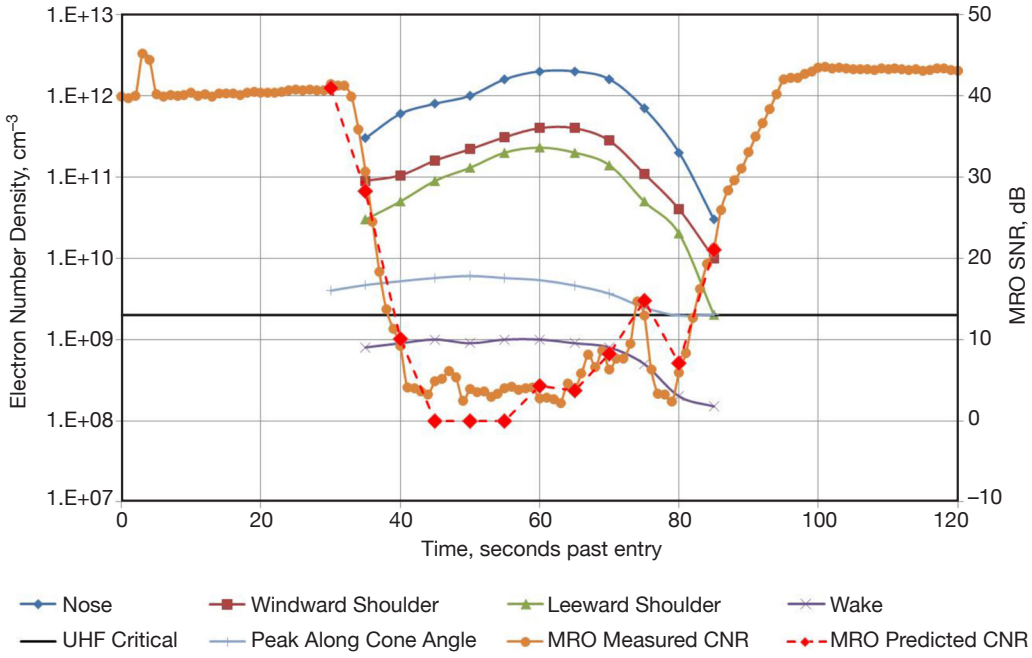

Figure 14. Same as Figure 12 except predicted CNRs (red diamonds) were made to agree with measured CNR by adjusting integrated electron density profile using multiplicative γ factors (shown in Figure 15).

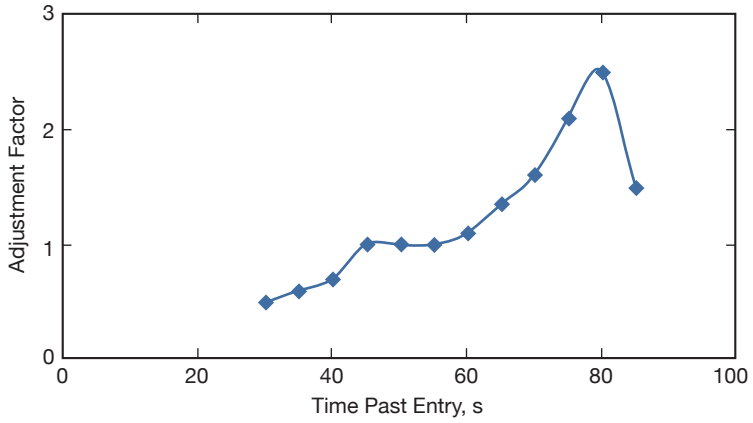

Figure 15. Multiplicative factors applied to electron number density profiles to allow agreement of predicted signal fades with measured fade signature for the MSL-to-MRO signal link (see Figure 14).

ing systematic trend in the multiplication factor from overestimation (factor below unity) to underestimation (factor above unity) crossing over somewhere between 45 s and 60 s (where there is total blackout due to huge fade values significantly exceeding the available signal CNR).

B. MSL-to-MEX Signal Link Analysis

For the MSL-to-MEX signal link, the domain of the LAURA computations extends about two to three aeroshell diameters into the wake region behind the capsule. Figure 16 shows the electron number density profiles along the line of sight at each time instance between t = 35 s and t = 85 s for this link. Figure 17 shows an electron number density color-coded contour plot along the line-of-sight extraction plane for the 50 s case. As the MSL-to-MEX signal paths generally lie in the wake direction, Figure 16 shows that all electron number density profiles lie below the UHF threshold value of 2×10^9 cm^{-3} required for signal degradation. However, these estimates are likely underestimated (as was the case with the MRO link) but at a much higher level. Some degree of signal degradation should be present as Figure 5 clearly shows the MSL-to-MEX link suffered significant degradation during the same period as the MSL-to-MRO link and the preflight prediction period. We thus utilize the attenuation correction factor (γ) analysis to match observed signal loss with predicted loss (see Figure 18).

The achieved attenuation factors for the MSL–MEX signal link (shown as red squares in Figure 18) also display a generally increasing trend, as do the MSL-to-MRO factors (blue diamonds). We are reminded that the uncertainties are higher at the extremities of the degradation period. The MSL–MEX factors are roughly two times higher than the MRO attenuation factors (blue diamonds), suggesting a higher degree of error in the electron number density estimates in the wake region. Future study would encompass a close examination of recombination and gas expansion models used in the LAURA analysis, allowing an improved estimation of electrons in the wake region.

C. Overview of MSL and Phoenix Signal-Level Profiles during Peak Heating Period

Figure 18 displays the attenuation correction factors for the three Phoenix orbiter relay links [1] and the two MSL orbiter relay links (MEX red, MRO blue). It should be emphasized that all adjustment factors shown in Figure 18 lie within the factor-of-10 uncertainty advertised for LAURA electron estimates and all links show systematic trends. We note the similarity of the attenuation factors and their trend for the three Phoenix (PHX) relay links, which all lie below unity, suggesting LAURA overestimated the electron number density for the Phoenix degradation period. For MSL, the MSL–MRO link displays factors that start out with overestimation trending to factors greater than unity, suggesting underestimation. From Figure 18, we see that the MSL–MEX attenuation factors lie at much higher values, suggesting significant underestimation of electron number density in the wake region. This could be explained by the fact that the errors in electron number estimation are higher in the wake region. The fact that the MSL trends near the end of the degradation period suggest underestimation of electrons, while those of the PHX trends suggest slight overestimation of electrons here, could be explained by different combinations of relative velocity and

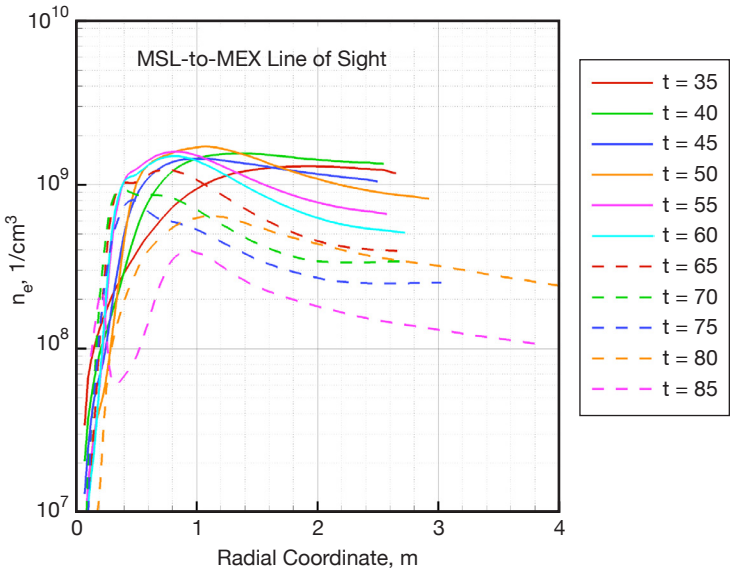

Figure 16. Electron number density profiles along the signal link at each time instance for the MSL-to-MEX signal link. The radial coordinate origin is at XLAURA = YLAURA = 0. The maximum electron number density of 1.8×10^9 cm^{-3} occurs at t = 50 s.

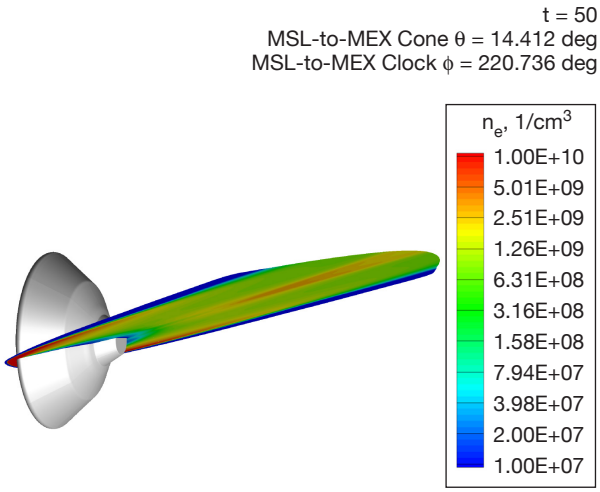

Figure 17. Electron number density color coded contour plot in the extraction plane for the MSL-to-MEX signal link occurring at t = 50 s past entry.

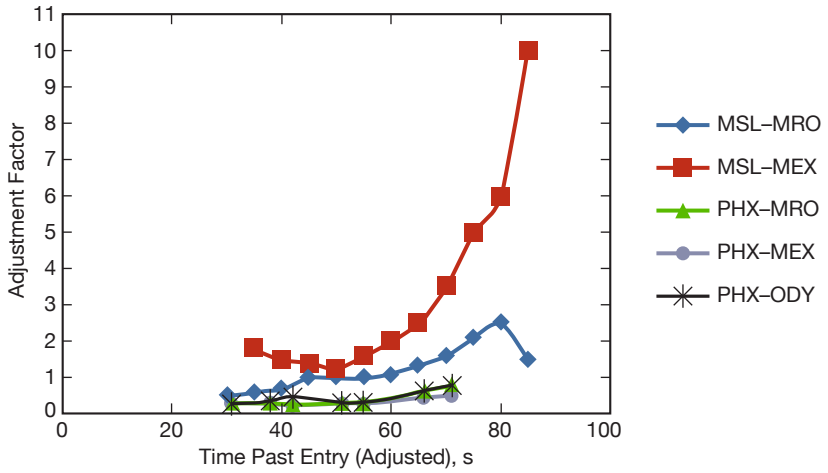

Figure 18. Multiplicative factors applied to electron number density profiles to force agreement of predicted signal fades with measured fades for the two MSL signal links and the three Phoenix signal links from [1]. Note that the time scale for Phoenix was adjusted as described in the caption for Figure 2.

neutral atmospheric density affecting the model outcomes differently. At the start of the degradation periods, the velocity is higher and the neutral air density is lower, while at the end of the degradation period the velocity is much lower and the density is higher, which contributes to electron generation. The subject of future study includes a revisit of the net effect of uncertainties due to LAURA and the trajectory in the different atmospheric regions. Such work would also involve varying LAURA models that are dependent on relative velocity and density to estimate electron number density profiles to match the degradation brownout results.

VI. Conclusion

The degradation periods for the MSL-to-MRO and MSL-to-MEX signal links are consistent with enhanced electrons along the signal path where the density exceeds the threshold density for degradation, well within the expected factor-of-10 uncertainty. The measured SNR degradation periods for both MRO and MEX orbiter links from MSL line up well with predicted electron number density curves as well as predicted signal levels (after adjustment) extracted from the electron number density profile along the signal path.

Acknowledgments

We would like to thank Allen Chen and Steven Sell of JPL for supporting this work, Jeremy Shidner of Langley Research Center for providing trajectory information and valuable data sets used in this analysis, Paula Brown of JPL for providing detailed PUHF antenna gain profiles used to correct measured signal-level estimates, and Peter Gnoffo of Langley Research Center for his well appreciated review of this article.

References

[1] D. Morabito, R. Kornfeld, K. Bruvold, L. Craig, and K. Edquist, "The Mars Phoenix Communications Brownout during Entry into the Martian Atmosphere," *The Interplanetary Network Progress Report*, vol. 42-179, Jet Propulsion Laboratory, Pasadena, California, pp. 1–20, November 15, 2009, and associated Errata (this issue). http://ipnpr.jpl.nasa.gov/progress_report/42-179/179A.pdf

[2] D. D. Morabito, "The Spacecraft Communications Blackout Problem Encountered during Passage or Entry of Planetary Atmospheres," *The Interplanetary Network Progress Report*, vol. 42-150, Jet Propulsion Laboratory, Pasadena, California, pp. 1–23, April–June 2002, cover date August 15, 2002. http://ipnpr.jpl.nasa.gov/progress_report/42-150/150C.pdf

[3] R. P. Kornfeld, M. D. Garcia, L. E. Craig, S. Butman, and G. M. Signori, "Entry, Descent, and Landing Communications for the 2007 Phoenix Mars Lander," *AIAA Journal of Spacecraft and Rockets*, vol. 45, no. 3, pp. 534–547, May–June 2008. dx.doi.org/10.2514/1.33789

[4] R. P. Kornfeld, K. N. Bruvold, D. D. Morabito, L. E. Craig, S. W. Asmar, and P. Ilott, "Reconstruction of Entry, Descent, and Landing Communications for the Phoenix Mars Lander, *AIAA Journal of Spacecraft and Rockets*, vol. 48, no. 5, September–October 2011.

[5] P. A. Gnoffo, R. N. Gupta, and J. L. Shinn, *Conservation Equations and Physical Models for Hypersonic Air Flows in Thermal and Chemical Non-Equilibrium*, NASA Technical Paper 2867, National Aeronautics and Space Administration, Hampton, Virginia, 1989.

[6] D. Morabito and K. Edquist, "Communications Blackout Predictions for Atmospheric Entry of Mars Science Laboratory," *Proceedings of the 2005 IEEE Aerospace Conference*, paper #1163, Big Sky, Montana, March 2005.

[7] A. R. Vasavada, A. Chen, J. R. Barnes, P. D. Burkhart, B. A. Cantor, et al., "Assessment of Environments for Mars Science Laboratory Entry, Descent, and Surface Operations," *Space Science Review*, pp. 793–835, May 2012.

[8] K. Oudrhiri, S. Asmar, P. Estabrook, D. Kahan, R. Mukai, et al., "Sleuthing the MSL EDL Performance from an X-band Carrier Perspective," *Proceedings of the 2013 IEEE Aerospace Conference*, pp. 1–13, Big Sky, Montana, March 2–9, 2013. http://ieeexplore.ieee.org/stamp/stamp.jsp?tp=&arnumber=6497418&isnumber=6496810

[9] M. Soriano, S. Finley, D. Fort, B. Schratz, P. Ilott, et al., "Direct-to-Earth Communications with Mars Science Laboratory during Entry, Descent, and Landing," *Proceedings of the 2013 IEEE Aerospace Conference*, pp. 1–14, Big Sky, Montana, March 2–9, 2013. http://ieeexplore.ieee.org/stamp/stamp.jsp?tp=&arnumber=6496816&isnumber=6496810

[10] C. Park, J. T. Howe, R. L. Jaffe, and G. V. Chander, "Revision of Chemical-Kinetic Problems of Future NASA Missions, II: Mars Entries," *Journal of Thermophysics and Heat Transfer*, vol. 8, no. 1, January–March 1994.

[11] A. Makovsky, P. Ilott, and J. Taylor, "Mars Science Laboratory Telecommunication System Design," Article 14, Deep-Space Communication and Navigation Systems Center of Excellence (DESCANSO) Design and Performance Summary Series, Jet Propulsion Laboratory, Pasadena, California, November 2009.
http://descanso.jpl.nasa.gov/DPSummary/Descanso14_MSL_Telecom.pdf